NimR Supplementary Data

```
HI_1623                  --MKIGALAKALGCTVETIRYYEQQGLIPPPKRTSGNFRQYNEEHLQRLS
Pseudo_CadR_[AAK48830]   --MKIGELAKATDCAVETIRYYEREQLLPEPARSDGNYRLYTQAHVERLT
HI_0293                  --MNISEAAKLVGLSTKQIRDYEKMGLIKPAVRSLSGYRNYGESDLERLH
Ecoli_CueR_P77565        --MNISDVAKITGLTSKAIRFYEEKGLVTPPMRSENGYRTYTQQHLNELT
Ecoli_ZntR_P36676        -MYRIGELAKMAEVTPDTIRYYEKQQMMEHEVRTEGGFRLYTESDLQRLK
Hinflu_HI0186_I64052     MTYTTAKAAEKIGISAYTLRFYDKEGLLPNVGRDEYGNRRFTDKDLQWLS
Ngono_NmlR_[NG0602]      MTYTTAKAAEKIGISAHTLRFYDKEGLLPNIGRDEYGNRCFTDNDLQWLY

                                                Dimerization helix
HI_1623                  FICNCRNLDISLSEIKSLLNLENASKQQ-AEEINRVLDKHIKEVATRIHE
Pseudo_CadR_[AAK48830]   FIRNCRTLDMTLDEIRSLLRLRDSPDDS-CGSVNALIDEHIEHVQARIDG
HI_0293                  FIRHSRNVGFSLHQIAQLLALQDNPKRS-CREVKVLTAQHIATLNQQIEQ
Ecoli_CueR_P77565        LLRQARQVGFNLEESGELVNLFNDPQRH-SADVKRRTLEKVAEIERHIEE
Ecoli_ZntR_P36676        FIRHARQLGFSLESIRELLSIRIDPEHHTCQESKGIVQERLQEVEARIAE
Hinflu_HI0186_I64052     LLQCLKNTGMSLKDIKRFAECTIIGDDT-IEERLSLFENQTKNVKCQIAE
Ngono_NmlR_[NG0602]      LLQCLKNTGMSLKDIKRFAECTVIGDDT-IEERLSLFENQIENVKCQIAE

                         Dimerization helix   Metal-binding  2-turn α-helix
                                                loop
HI_1623                  LAHLRMKLIELREKTVSN-DEDPMKLLLQHSGVKFVRLK-----------
Pseudo_CadR_[AAK48830]   LVALQEQLVELRRRCNAQGAECAILQQLETNGAVSVPETEHSHVGRSHGH
HI_0293                  LQKMVQKLQHWHDSCQG--NDNPECLILNGLNG-----------------
Ecoli_CueR_P77565        LQSMRDQLLALANACPG--DDSADCPIIENLSGCCHHRAG----------
Ecoli_ZntR_P36676        LQSMQRSLQRLNDACCGTAHSSVYCSILEALEQGASGVKSGC--------
Hinflu_HI0186_I64052     LK----RYLDLLEYKLAFYQKAKALGSVKAVNLPQIPETS----------
Ngono_NmlR_[NG0602]      LK----RYLDLLEYKLAFYQKAKALGSVKAVNLPQIPETA----------
```

Fig. S1. The alignment of protein sequences of members of the MerR Family. The MerR-like regulators present within *H. influenzae* (HI0293, HI1623/*nimR* and HI0186/$nmlR_{hi}$) are aligned against members of the MerR family of known structure (CueR and ZntR) and, given the annotation of HI1623 as CadR, the Pseudomonas CadR is included.

Table S1: The known nickel co-factored enzymes present in *H. influenzae* Rd KW20.

Nickel co-factored protein	***H. influenzae* homolog**
hypA- nickel insertion into hydrogenase 3	No homolog
hypBDEF - GTP hydrolase involved in nickel liganding into hydrogenases	No homolog
hypG - hydrogenase 2 accessory protein	No homolog
nikR – nickel regulator of *nikABCDE*	No homolog
nikABCDE – nickel uptake	No homolog
nixA - high-affinity nickel-transport protein	No homolog
hupUV - uptake hydrogenase accessory protein	No homolog
hoxAB -	No homolog
CODH – carbon monoxide dehydrogenase	No homolog
ACDS acetyl-coA decarboxylase/synthase	No homolog
ureAB	HI0540-HI0541
ureC-H	HI0535-HI0540
Acetyl coA carboxylase	No homolog
Methyl CoM reductase	No homolog
Ni-SOD	No homolog
Dioxygenase	No homolog
Glyoxylase A – *gloA*	HI0323
Cca; tRNA nucleotidyltransferase	HI1606
nicO - high-affinity nickel-transporter/efflux	NiCoT homolog HI1248

Table S2: Analyses of Ni(II) content in NimR using excess PAR in the absence (-) and presence (+) of 8 M urea.

Fraction mL	[NimR] µM		[Ni] µM		[Ni]/[NimR]	
	-	+	-	+	-	+
4	6.27	6.27	2.74	2.67	0.44	0.43
4.5	7.26	7.26	3.55	3.58	0.49	0.49
5	6.95	6.95	4.07	4.13	0.59	0.59
				Average	0.50 ± 0.07	
4[a]	3.06	3.06	1.50	1.52	0.49	0.50
4.5[a]	5.98	5.98	2.56	2.51	0.43	0.42
5[a]	6.55	6.55	3.16	3.31	0.48	0.51
				Average[a]	0.48 ± 0.04	

[a] NimR was incubated with Ni(II) in the presence of 0.5mM glycine prior to elution on PD-10 column.

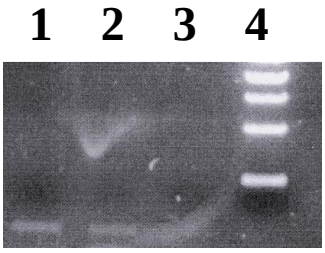

Fig. S2. The *nikKLMQO* genes form an operon. RNA was extracted from *H. influenzae* Rd KW20 using a QIAGEN RNeasy Mini Kit (QIAGEN). RNA was quantified using its absorbance at 260 nm and was checked for DNA contamination by PCR (lane 3). Prior to the RT reaction, RNA was further treated to remove any residual DNA using Promega DNase (Promega Corp., USA). The RT reaction was performed using the QIAGEN Omniscript Reverse Transcriptase Kit (QIAGEN, USA). Primers were used from HI1618 (*nikO*) (rtnikO: 5'TTGCCGAACTGAAAACCA) and HI1621 (*nikM*) (rtnikM: 5'-TCGTACCGAGAATTTCTC); HI1621 (rtnikM2: 5'AACACGCCTTCAGATAAATGCAT) and HI1624 (*nikK*) (rtnikK: 5'GTGGAATATATGCTAAC). PCR was carried out with New England Biolabs Taq Polymerase (NEB, USA). RT-PCR is shown for *nikK-nikM* (lane 1) and *nikM-nikO* (lane 2). Lane 4 is size marker.

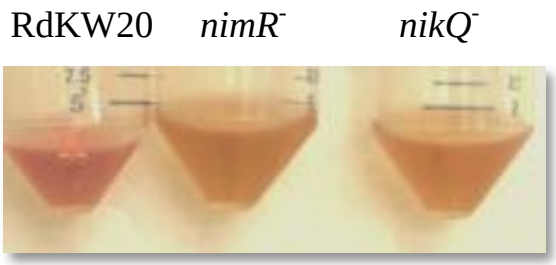

Fig. S3. The *nimR* and *nik* genes are required for maintaining pH during *H. influenzae* growth. The pH is indicated in CDM by the presence of phenol red, a dye which is yellow in solution with a pH below ~6.8 and then changes colour from red to pink as the pH increases to 8.2. The pH is indicated in the spent media and is seen to decrease in the *nimR* and *nikQ* mutant strains (yellow) compared to the wild type Rd KW20, where the pH is maintained above pH6.8.

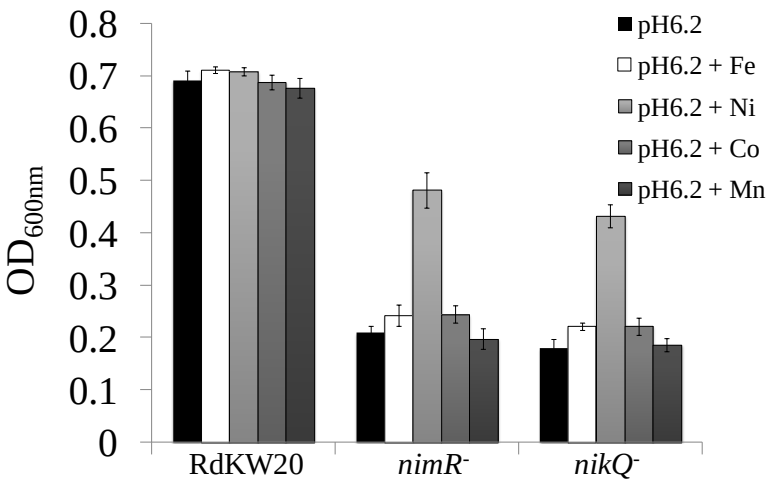

Fig. S4. The growth defect at pH6.2 of the *nimR* and *nikQ* mutant strains can be recovered specifically by the addition of excess Ni(II). Each of the wild type RdKW20, *nimR* and *nikQ* strains were grown at pH 6.2 in CDM and then with the addition of particular metal ions and the end point (24h) of growth was noted (OD_{600nm}).

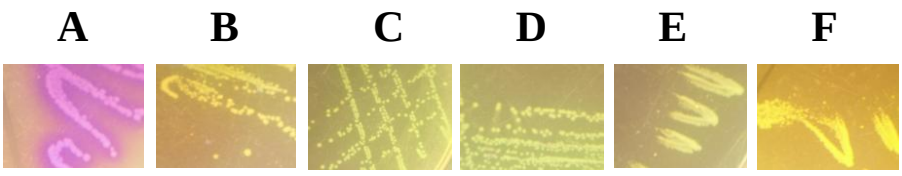

Fig. S5. Urease activity in *H. influenzae* requires the *nik* operon for the import of Ni(II). In urease overlay assays the wild type Rd KW20 displayed activity (shown by the pink colour, panel A), while the *nikQ* mutant had no urease activity (panel B) and in contrast to the addition of Ni(II) (Fig. 3) this could not be rescued by addition of Fe(II) (panel C), Co(II) (panel D) or Mn(II) (panel E). The addition of the urease-specific inhibitor flurofamide confirmed the activity in the assay was being expressed by urease; there was no activity in the presence of this specific inhibitor (panel F).

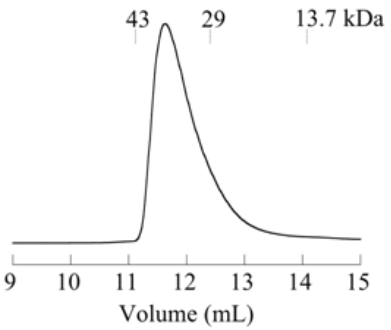

Fig. S6. Elution of purified NimR on a Superdex 75 analytical size exclusion column (H10/30; GE Healthcare). NimR was eluted at ambient temperature using HEPES buffer (25 mM; pH 7.0) containing NaCl (150 mM) at a flowrate of 0.7 mL/min. The elution volumes of size standards are shown (ovalbumin, 43 kDa; carbonic anhydrase, 29 kDa; ribonuclease A, 13.7 kDa; GE Healthcare).

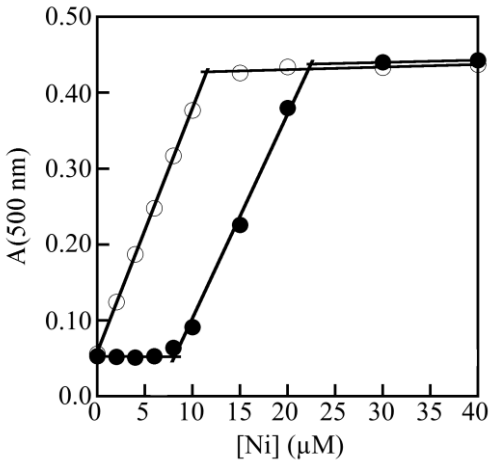

Fig. S7. Equilibrium binding competition between PAR and NimR for Ni(II) as monitored by the absorbance of the $Ni^{II}(PAR)_2$ complex at 500 nm (ε ~ 40000 M^{-1} cm^{-1}). All titrations were performed in HEPES buffer (50 mM; pH 7.4) containing 150 mM NaCl. Empty circles (○): nickel(II) chloride was titrated into a solution of PAR (24 μM) in the absence of an equimolar amount of NimR (24 μM). This curve demonstrated that NimR did not compete with PAR for Ni(II) under these conditions. An identical curve was obtained when Ni(II) was titrated into a mixture of PAR (24 μM) and EGTA (8 μM), providing a lower limit for the affinity of PAR to Ni(II) ($\beta_2 > 10^{13.5a}$). Filled circles (●): nickel(II) chloride was titrated into PAR (24 μM) in the presence of EDTA (8 μM). This curve showed that EDTA bound Ni(II) more strongly than did PAR, thus providing an upper limit for the affinity of PAR to Ni(II) ($\beta_2 < 10^{18.6a}$). Taken together with the pseudo-competition experiment with glycine as described in text, the affinity of NimR to Ni(II) could be estimated to lie within the range: $K_A(Ni^{II})$: glycine ($10^{10.8a}$) < NimR ≤ EGTA ($10^{13.5a}$) < PAR < EDTA ($10^{18.6a}$) ([a] from Martell and Smith. *Critical Stability Constants*, New York: Plenum Press, **1989**).

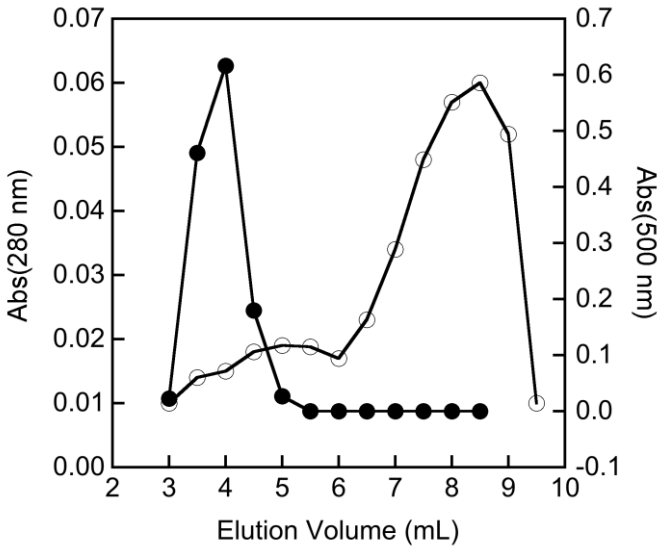

Fig. S8. NimR does not bind Zn(II). Elution of a mixture of NimR and excess zinc sulfate (1.1 equiv) on a PD-10 column (GE Healthcare) in 50mM HEPES buffer (pH 7.2) containing 150mM NaCl. Eluted fractions were analysed for NimR (filled circles) by measuring the solution absorbance at 280nm and for Zn(II) (empty circles) by reaction with excess PAR (40µM) and measuring the solution absorbance at 500nm due to the $Zn(PAR)_2$ complex.